

Improved accuracy of γ -ray intensities from basic principles for the calibration reaction $^{14}\text{N}(n, \gamma)^{15}\text{N}$

T. Belgya

Institute of Isotopes Hungarian Academy of Sciences, POB 77, H-1525 Budapest, Hungary

(Received 17 June 2005; revised manuscript received 28 February 2006; published 22 August 2006)

The $^{14}\text{N}(n, \gamma)^{15}\text{N}$ reaction is a primary source of high-energy γ rays for use in the calibration of detectors for other neutron-capture reactions. The γ -ray intensities of ^{15}N produced by thermal neutron capture and the γ -ray detection efficiency function have been simultaneously determined from γ -peak areas alone using the basic principle of intensity balance. A least-squares fit was made to a new type of intensity balance calculation, combined with traditional efficiency fitting of radioactive sources. This latter ensures the compatibility with low-energy efficiencies, while providing an unbiased efficiency function for higher (up to 10 MeV) γ -ray energies. The calculation is based on the assumption that the ^{15}N decay scheme is complete. From the internal consistency of the resulting intensities, it is believed that they are more accurate than previously published values. The same is true for the derived efficiency function.

DOI: [10.1103/PhysRevC.74.024603](https://doi.org/10.1103/PhysRevC.74.024603)

PACS number(s): 25.40.Lw, 23.20.Lv, 29.25.Rm, 29.30.Kv

I. INTRODUCTION

The full energy peak efficiency (FEPE) calibration of modern germanium γ -ray detectors in the energy range of 0.1–10 MeV is a long-standing problem [1–5]. To determine the FEPE one needs to have radioactive sources with precisely known intensities. Unfortunately the commonly available, well-calibrated sources only go up to a γ energy of 2.7 MeV (^{24}Na source). To determine intensities for higher energy sources, one would need a good efficiency calibration and vice versa, so Raman *et al.* accurately characterized this problem as the chicken-egg dilemma [2].

An accurate and precise knowledge of the FEPE is needed to calculate a large variety of important nuclear data from experimental data. These important nuclear data quantities include the thermal-neutron and other reaction cross sections based on γ -ray spectroscopy. The uncertainty in the FEPE also affects the precision of many nuclear analytical methods, radiation dose calculations and measurements generated by high-energy γ rays, and even the results of any planetary prompt γ activation analysis (PGAA) [6–8]. There are also medical, nuclear waste management [9], nuclear astrophysics [9], and safeguard applications [10,11] that are affected. Thus, it is important to obtain independent results for the intensities of the higher energy calibration sources to be used in FEPE determinations.

At low γ -ray energies, there are sources with sufficiently simple level schemes for which absolute decay probabilities can be determined from level scheme considerations, or there are single γ -ray sources whose activities can be determined by absolute methods, such as $4\pi\beta\gamma$ counting [2]. For sources with two consecutive γ rays with 1:1 intensity ratios, the higher energy FEPE can be inferred from the lower energy FEPE [1]. This method, however, works only up to 2.7 MeV. Above this energy, only multi- γ -ray sources are available, like ^{56}Co and ^{66}Ga [2,12]. However, it was reported recently that their intensities are in error above 2.7 MeV because of erroneous extrapolations of the detector efficiency curves used in their intensity measurements [12,13]. This observation

caused experts to review and update the IAEA recommended calibration standards [14]. This work has been finished recently and summarized by Nichols [10], and the most commonly used radioactive source data from that recent evaluation are listed in Ref. [15].

For even higher energies, only nuclear reactions such as (n, γ) or (p, γ) can produce γ cascades with 1:1 intensity ratios. Furthermore, capture reactions have only one source, the capture state, which is fed directly by the reaction, while other reactions such as $(n, n'\gamma)$ or $(p, p'\gamma)$ excite several states at once, so they have several source levels. Decay scheme considerations are much easier to use for the single-source-level reactions. From the capture state, γ -ray cascades lead to some drain level, which is the ground state. The (p, γ) reaction in general suffers from the uncertainty caused by the angular correlation [16], unlike the simpler case of the thermal neutron (n, γ) reaction, where the captured neutron is usually in an s state. This favors the (n, γ) reactions for producing high-energy, high-precision calibration sources based on decay scheme considerations.

Light nuclei have very simple level schemes; however, their partial γ -ray production cross sections are usually extremely low, which make them unsuitable for being an easy to use source. The lightest nucleus with sufficient neutron-capture cross section is ^{14}N [2]. Thermal neutron capture on ^{14}N results in a relatively simple decay scheme in ^{15}N . While ^{15}N produced in the (n, γ) reaction is considered to be a primary source, the procedure previously used to determine the ^{14}N capture intensities is described as a long and painful iterative process by Journey *et al.* [3,17]. This makes it urgent to obtain new, independent intensity data and to discover a new procedure for obtaining the detector efficiency. The only previous effort at performing a real least-squares fit to the intensity balance calculations for the ^{15}N neutron-capture decay scheme was made by Kennett *et al.* [4], but they used only pair spectrometer data, leaving out the low-energy γ transitions. The most complete data for the ^{15}N capture decay scheme was published a decade later by Journey *et al.* [3]; 30 new and previously undetected weak γ rays were placed in

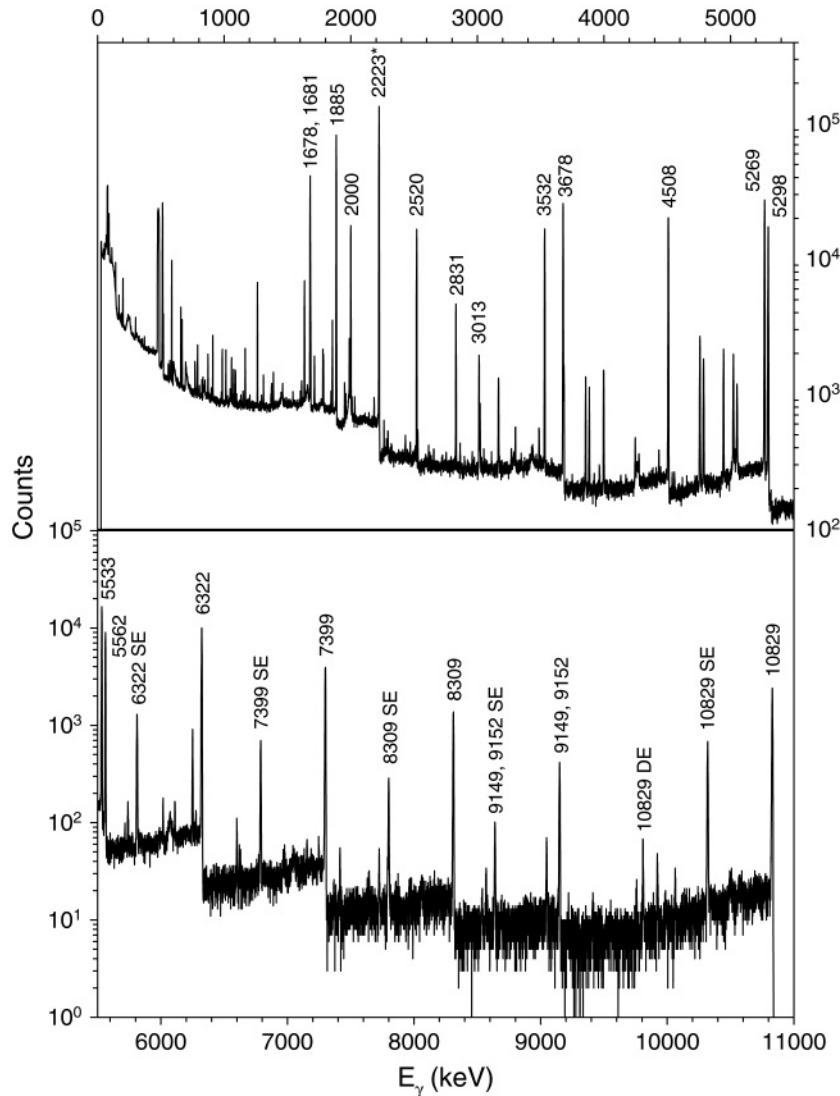


FIG. 1. Compton suppressed urea-d (n, γ) spectrum. Upper curve shows the low-energy part of the spectrum, corresponding scale is on the right. Lower curve is the high-energy part, scale is on the left. The most intense $^{14}\text{N}(n, \gamma)^{15}\text{N}$ γ lines are labeled with their energies. SE or DE denote the single- or double-escape peaks. Star (*) shows the hydrogen capture line.

their decay scheme. A very recent work in Japan has confirmed these results [5].

In this article, we report a least-squares fit to a new kind of intensity balance calculation (named crossing intensity sum or CIS) applied to γ rays observed in our experiments performed with cold neutron capture on ^{14}N at the Budapest PGAA-NIPS facilities [18–21]. NISP is an acronym for Neutron Induced Prompt-gamma-ray Spectroscopy. Some preliminary results were presented at the 12th International Conference on Capture Gamma-Ray Spectroscopy and Related Topics [22]. The details of this new analysis method will be published elsewhere. As we will see below, the Ge detector efficiency and the γ -ray intensities were obtained directly from the measured peak areas utilizing this new method.

II. EXPERIMENTS

The neutron-capture experiments using urea-d (ND_2COND_2) were performed at the PGAA-NIPS facilities of the Budapest research reactor. Since the whole system was previously described [18–21], we give here only a brief description. For γ -ray-singles experiments the PGAA

experimental station was used. It consists of an evacuated target chamber in which the cold neutron flux was measured to be $5 \times 10^7 n/s \text{ cm}^2$ at the target position. The beam size was limited to $2 \times 2 \text{ cm}^2$ by a set of collimators. A mass of 1.194 g of urea-d powder was put into a thin Teflon bag of $2 \times 3 \text{ cm}^2$ area to minimize γ -ray absorption. The bag was held in an aluminum frame between thin Teflon strings. The frame had an angle of 30° relative to the impinging neutron direction. The 25% efficiency, collimated and Compton-suppressed HPGe detector was set perpendicular to the beam direction, and its end cap was 23 cm from the center of the sample. This standard setup ensures negligible ($< 0.1\%$) true coincidence summing. An experiment with a 2 mm thick and 2 cm diameter pressed pellet of urea-d was also performed to determine the contribution of the Teflon bag. The $^{14}\text{N}(n, \gamma)^{15}\text{N}$ spectrum taken for about 264 000 s is shown in Fig. 1. The count rate was about 43 counts per second (cps) with negligibly low dead time. This spectrum was used for the new crossing intensity sum fitting. The usual background rate for this setup is about 4 cps. The background has already been studied in detail, and the results are being published [23].

γ - γ coincidence experiments were also done using the pressed pellet to obtain placement information in the decay scheme. The sample was placed in the sample holder of the NIPS station, and its surface was set to 30° relative to the impinging neutron beam. In these experiments, a 13% and a 30% HPGe detector were placed close to the target at 90° to the neutron beam. A detailed description of the coincidence setup can be found in Ref. [21]. The data were collected in list mode for about 5 days, which yielded about 7.6 million events in the time-integrated spectra. The energy gates were applied on the 30% detector to obtain a projection for the 13% detector. Peak intensities down to about 1% of the most intense peak could be observed in this way.

To obtain reliable results for the low-energy efficiency, we included efficiency data determined for each recommended peak from measurements performed on radioactive sources. We used commercial ^{60}Co , ^{133}Ba , ^{152}Eu , and ^{207}Bi standard radioactive sources and homemade $^{110}\text{Ag}^m$ and ^{182}Ta sources.

III. PREPARATION OF DATA FOR EFFICIENCY FITTING

All of the measured spectra used in this work were evaluated with the HYPERMET PC program package [24–27] developed in our department. This program provided peak areas and positions, as well as their statistical uncertainties.

The identification of background peaks is based on direct comparison of the nitrogen spectra with spectra taken from possible background components [23]. The contributions from these, including the single-escape(SE) and double-escape(DE) peaks, were directly subtracted from the ^{15}N peak areas. The very low, but not negligible γ -ray absorption and neutron absorption were calculated with numerical integration, and the corresponding corrections made to the net peak areas. A list of the identified ^{15}N γ peaks and their absorption- and interference-corrected net peak areas are presented in Table I. Three weak γ rays (at 608.3, 2002.3 (close doublet with 1999.7), and the 10697.8 keV) could not be observed out of the 58 γ rays reported by Journey *et al.* [3]. However, one additional γ ray, the 977.2-keV transition reported in the Evaluated Nuclear Structure Data File (ENSDF) [28], was detected. Though the very weak 383 keV γ ray has been observed, no deexciting transition could be identified from the 10450 keV level, similar to the findings of Journey *et al.* [3].

The close doublet at 9150 keV could not be resolved in the singles spectrum, but we tried to resolve them in the coincidence spectra. The coincidence experiment suggests a 10 to 1 ratio for the 9149 and 9152 keV peak areas with about 40% uncertainty on the smaller area.

Most importantly, we did not perceive the 10697 keV transition from the proton unstable 10702 keV level, but observed its weak feeding 131 keV transition. Contrary to Journey *et al.* [3], we believe that its γ -branching ratio is so small relative to the proton decay branching that it is impossible to detect. This is also confirmed by the results of Warburton *et al.* [29]. By summing up all of our $^{14}\text{N}(n, \gamma)$ spectra, we were not able to discover it. Therefore, we left out the 131 and 10697 keV transitions from the fitting procedure described below. They would not noticeably influence the crossing intensity sum calculations because most

TABLE I. γ -ray energies and net corrected peak areas (in counts) of ^{15}N excited in thermal neutron-capture reactions.

| E_γ (keV) | Net area | Comments |
|------------------------|-------------|--|
| 131.4(1) | 2251(249) | |
| 382.4(15) | 159(147) | |
| 583.6(10) ^a | 6916(444) | ^{20}F yield is subtracted |
| 767.8(1) | 2251(122) | |
| 770.3(5) | 217(98) | |
| 831.1(3) | 814(96) | |
| 908.4(1) | 5164(129) | |
| 977.2(5) ^a | 376(161) | ^{20}F yield is subtracted |
| 1011.7(1) | 3985(117) | |
| 1025.1(3) | 289(83) | |
| 1053.5(2) | 519(67) | |
| 1073.0(1) | 2244(80) | |
| 1610.7(1) | 1575(100) | |
| 1678.2(1) | 147853(510) | |
| 1681.2(1) | 30199(266) | |
| 1783.5(2) | 4279(242) | |
| 1854.0(1) | 10740(145) | |
| 1884.8(1) | 313797(531) | |
| 1988.6(1) | 6158(194) | |
| 1999.6(1) | 64647(262) | |
| 2030.6(1) | 1367(135) | |
| 2247.6(3) | 261(66) | |
| 2261.9(1) | 1111(72) | |
| 2293.4(8) | 689(68) | |
| 2520.3(1) | 71426(289) | |
| 2724.5(4) | 280(69) | |
| 2830.7(1) | 19754(122) | |
| 2898.2(4) | 321(56) | |
| 3013.4(2) ^a | 7540(130) | ^{20}F yield is subtracted |
| 3269.2(2) | 498(60) | |
| 3300.6(1) | 1332(193) | |
| 3531.8(1) | 83617(316) | |
| 3677.5(1) | 128432(428) | |
| 3855.3(2) | 6248(117) | |
| 3880.8(4) | 475(107) | |
| 3884.0(2) | 4800(138) | |
| 3923.1(4) | 230(100) | Yield of ^{13}C 4945 keV DE is subtracted |
| 4508.4(1) | 116135(470) | |
| 4653.7(5) | 182(46) | |
| 5268.7(1) | 170764(501) | |
| 5297.4(1) | 120068(833) | |
| 5533.0(1) | 105005(481) | |
| 5561.6(1) | 57083(287) | |
| 6322.0(2) | 81222(379) | |
| 7153.1(3) | 226(28) | |
| 7298.4(3) | 33370(169) | Yield of 8309 keV SE is subtracted |
| 8309.4(3) | 11793(114) | |
| 8567.7(5) | 190(16) | |
| 9045.7(6) | 460(29) | |
| 9148.0(4) ^b | 3783(68) | |
| 9218.6(5) | 64(11) | |
| 9755.2(7) | 141(17) | |
| 9919.8(8) | 280(25) | |
| 10059.8(6) | 158(24) | |
| 10829.1(5) | 22506(162) | |

^aEnergy uncertainty is increased due to a major contribution from a contaminating peak.

^bArea of this peak is distributed in a 10:1 ratio (3439 and 344) for the 9149 and 9152 keV peak areas in the decay scheme, respectively.

of the intensity found in the 131 keV transition would feed the unobserved ^{14}C and not other states in ^{15}N . The 10 450 keV level, fed by the 382 keV transition, was also taken out from the fit, because of the missing deexciting transitions and their very small contribution to the crossing intensity sums.

Otherwise, the decay scheme we used agrees with the decay scheme of Journey *et al.* [3] and the one in the recent ENSDF [28]. For the CIS calculation, we used all of the 136 possible transitions between the considered 17 levels, except for four transitions below 100 keV, because they are unobserved and improbable; in addition, the detector efficiency calculations were not considered below that energy. We also excluded the primary transition to the ground state, because its intensity is not related to that of any other γ ray, and hence its intensity cannot be determined by this procedure. Upper limits for the peak areas of the undetected transitions were estimated from the spectrum using Currie's detection limit [30]. In the CIS calculations, zero area was assumed for each unobserved γ ray with an uncertainty equal to the value of the detection limit.

The data from the radioactive sources were used to calculate the low energy ($0.1 \text{ MeV} < E < 1.8 \text{ MeV}$) efficiency function of our HPGe detector using the HYPERMET PC efficiency subroutine [1,26]. In the calculations, the latest recommended intensities [10,15] were used for each radioactive source.

IV. LEAST-SQUARES FIT OF EFFICIENCY AND DETERMINATION OF INTENSITIES

A brief description of the new crossing intensity sum (CIS) method is given here. Let us consider a decay scheme of a nucleus with a number of levels n up to and including the capture state (see Fig. 2, with $n = 5$). The arrows represent all of the possible γ decay in the decay scheme. In this model, the γ source is the capture state, the drain is the ground state, and the crossing intensity sums represent the continuity equations for this discrete problem. We will call a decay cascade any decay path which connects the capture state to the ground state with a consecutive series of two or more nonparallel transitions (see thicker arrows in Fig. 2.). First we prove that the sum of γ -ray intensities crossing any single line between

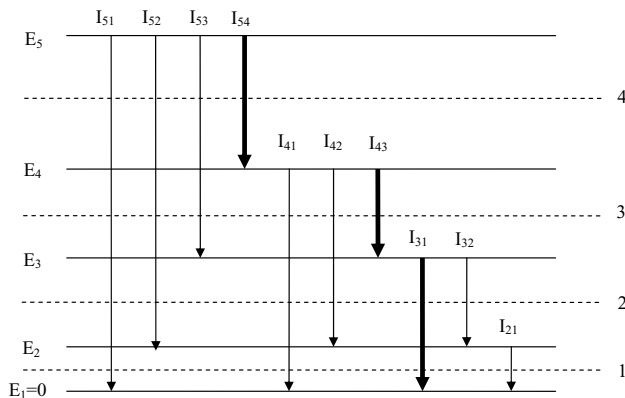


FIG. 2. Simplified decay scheme to demonstrate the CIS concept. Dashed lines are crossing lines, arrows represent transitions between states. Intensities of arrows passing through a crossing line must be summed to obtain the crossing intensity sum for that crossing line.

any two neighboring states (see dashed lines in Fig. 2) is a constant C . The crossing intensity means the intensity of a γ ray, which crosses a dashed line, and the crossing intensity sum is the sum of all such crossing intensities for a given dashed line.

Without going into complicated mathematics, it is easy to see that for any one decay cascade, e.g., as drawn with thicker arrows in Fig. 2, going from the capture state to the ground state will increase each of the $n - 1$ crossing intensity sums by 1 (the intensity of one photon is 1). Due to the statistical nature of the decaying process, different paths are realized from one excitation of the capture state ($E5$ in Fig. 2) to the next, but transitions belonging to each decay cascade path will increase each crossing intensity sum by 1. Thus, if we repeat the capture excitation C times, then the value of each of the $n - 1$ crossing intensity sums will be C . We mention here that the constancy of the crossing intensity sums can also be proved with the intensity balance principle and mathematical induction, but it is rather lengthy and thus we will give it elsewhere.

The experimental intensity $I_{i,j}$ of a certain γ ray deexciting level i and feeding level j can be expressed with the inverse FEPE $\varepsilon^{-1}(E_{i,j})$ and the corrected peak area $A_{i,j}$ as

$$I_{i,j} = A_{i,j} \varepsilon^{-1}(E_{i,j}) \quad (1)$$

The corrected peak area can be obtained from the measured γ -ray peak area $A'_{i,j}$ by correcting it for the self-absorption in the sample, for the electron conversion and pair conversion events that are not detected in our case. Strictly speaking, the intensity $I_{i,j}$ represents the total electromagnetic decay including the γ -ray intensity and the electron conversion and pair conversion intensities. In our case, both the electron conversion and the pair conversion corrections are negligible. The equations can be generalized for transitions including other particle decays, but we will not consider them in this article.

To simultaneously find out the unknown intensities and the detector efficiency function, we can utilize the CIS method. Instead of solving the direct CIS equations

$$\sum_{\substack{i>f \\ j<f}} I_{i,j} = \sum_{\substack{i>f \\ j<f}} A_{i,j} \varepsilon^{-1}(E_{i,j}) = T'_f = C \quad (2)$$

$$f = 1, 2, \dots, n - 1,$$

which can be over determined, we minimize a least-squares function, which is set up using the inverse efficiency for both the γ lines of the radioactive sources and the crossing intensity sums. In Eqs. (1) and (2), the indexes i and j denote the initial and final state numbers, while index $f = 1, 2, \dots, n - 1$ runs over all of the crossing lines. Before setting up the least-squares function, we define the vector T with elements $T_f = T'_f - C$, which has 0 mean for all of its components. Because the T_f values are not independent, we have to use their variance-covariance matrix \underline{w} as a weighting factor in the least-squares function. Its elements can be calculated in the following way

$$w_{f,k} = \langle \delta T_f \cdot \delta T_k \rangle = \left\langle \left(\sum_{\substack{i>f \\ j<f}} \delta I_{i,j} - \delta C \right) \left(\sum_{\substack{l>k \\ m<k}} \delta I_{l,m} - \delta C \right) \right\rangle, \quad (3)$$

here the bra-ket means averaging of statistical variables, and the δ operator means the difference of the statistical variable and its mean value. Since C is a constant, $\delta C = 0$, and we obtain

$$w_{f,k} = \sum_{\substack{i>j \quad l>k \\ j\leq j \quad m\leq k}} \langle \delta I_{i,j} \cdot \delta I_{l,m} \rangle, \quad (4)$$

The uncertainties of the intensities ($\delta I_{i,j}, \delta I_{l,m}$) which appear in Eq. (4) can be estimated using the corrected peak-area uncertainties multiplied by the corresponding inverse efficiency calculated from the known literature intensities. Since we expect that the new, unknown inverse efficiency—which we will determine—will not differ very much from the inverse efficiency calculated from the literature values, this will be a good first approximation for calculating the intensity uncertainties. Iterations of the least-squares procedure with the new intensities in a self-consistent manner can make it independent of the literature values. From here, the calculation of Eq. (4) is straightforward, because the measured peak areas are independent, that is,

$$\langle \delta I_{i,j} \cdot \delta I_{l,m} \rangle = \begin{cases} (\delta I_{i,j})^2 = (\delta A_{i,j} \hat{\varepsilon}^{-1}(E_{i,j}))^2, & \text{if } i = l \\ & \text{and } j = m, \\ 0, & \text{else,} \end{cases} \quad (5)$$

and $\hat{\varepsilon}^{-1}(E_{i,j})$, an approximate fixed inverse detector efficiency function taken from another experiment, is used to avoid the nonlinear feature of the least-squares equation. Now we can set it up as

$$\chi^2 = \sum_{\substack{1 \leq f \leq n-1 \\ 1 \leq k \leq n-1}} T_f w_{f,k}^{-1} T_k + \sum_m \frac{(\hat{\varepsilon}_m^{-1} - \varepsilon^{-1}(E_{i,j}))^2}{\sigma_m^2}. \quad (6)$$

The least-squares function consists of two terms. The first represents the CIS principle, and the other uses radioactive sources to fix the low-energy efficiency, where there are no strong transitions in the $^{14}\text{N}(n, \gamma)$ reactions. In this way, we can obtain a functional representation of the detector efficiency and determine the intensities at the same time. In our concrete case, the intensities $I_{i,j}$ belong to the electromagnetic transitions deexciting ^{15}N , $\varepsilon^{-1}(E_{i,j})$ is the unknown inverse detector efficiency function, the $\hat{\varepsilon}_m^{-1}$ is the m th inverse detector efficiency value determined from one of the corresponding radioactive source γ lines and σ_m^2 is its uncertainty. In a previous article, we already showed that the inverse efficiency of an HPGe detector can be well represented as a cubic spline [31]. Thus, by determining the linear coefficients of the cubic spline fit, we can obtain a good representation of the efficiency function, and hence of the electromagnetic transition intensities, in the least-squares fit procedure. In this work, we used a cubic spline with nine linear coefficients as in Ref. [31]. More details about the CIS procedure will be published later.

The least-squares fit to the FEPE was performed with a program named CUBICEFFI in which we implemented the procedure outlined above, which is based on the basic principle of CIS. The calculated FEP efficiency (full line) is shown in Fig. 3 and is compared with our usual efficiency fit (dotted line) to our peak areas, $A'_{i,j}$, divided by the intensities of Journey

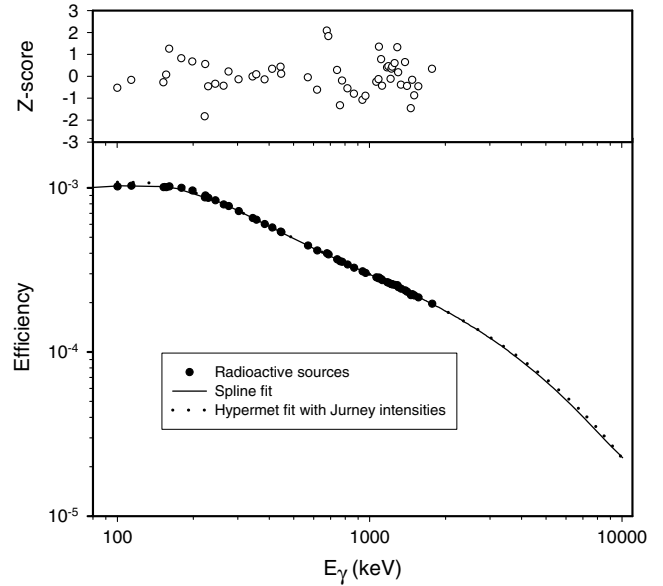


FIG. 3. FEP efficiency obtained from least-squares fit to radioactive source intensities and the ^{15}N crossing intensity sums. Solid circle symbols are experimental efficiency values measured with radioactive sources. Solid line represents the fit based on the principle of CIS. Dotted line is the efficiency fit to the same radioactive source and $^{14}\text{N}(n, \gamma)^{15}\text{N}$ data with the efficiency subroutine of the HYPERMET PC program, but the intensities of Journey *et al.* [3] were used to calculate the efficiency from the peak areas we obtained for the $^{14}\text{N}(n, \gamma)^{15}\text{N}$ reactions.

et al. [3] using the HYPERMET PC [1,26] efficiency subroutine. The upper panel shows the Z score of the fit for those points obtained from the measured data for the radioactive sources. Here we do not expect difference between the two calculations, and the Z score shows really no difference.

The calibration sources were selected to minimize the overlap between the strong nitrogen transitions. Indeed, the highest γ -ray energy from the radioactive sources is at 1770 keV, which barely overlaps with the strong 1678 and 1681 keV transitions; above this energy, radioactive sources have only a minor influence on the efficiency values.

The number of degrees of freedom of the fit can be calculated from the number of data values (52) belonging to the radioactive sources plus the number of crossing intensity sums (16) minus the number of free parameters ($9 + 1$). The resulting reduced χ^2 is 0.73, which is rather close to the expected 1. Nevertheless, the efficiency curve uncertainty was determined from the uncertainties of the original Budapest input data without adjusting their values to obtain the expected χ^2 value of 1. An iteration of the least-squares procedure was also done, replacing the approximate efficiency used to calculate the intensity uncertainties with the newly determined efficiency and making the calculation independent of the literature nitrogen intensities. This hardly changed the result and yielded reduced χ^2 of 0.72, so further iteration was not performed. The influence of the neglected pair conversion [32] was determined performing the correction; but the change was only 0.05%, so we decided to keep the result with no correction, because the uniqueness of the correction could

TABLE II. Intensity values of the strongest γ rays used for detector calibration from the $^{14}\text{N}(n, \gamma)^{15}\text{N}$ reaction. Intensities in this work are normalized using the recently measured elemental partial γ -ray cross section of 14.52(7) mb for the 1885 keV γ ray by Révay *et al.* [33]. To calculate the isotopic cross sections, we corrected for the isotopic abundance of ^{14}N (99.632%). Statistical uncertainty values of this work have been increased by 0.5% in quadrature in order to account for the neglected pair conversion correction and for the absorption correction uncertainty.

| E_γ (keV) | I_γ (mb) Jurney <i>et al.</i> [3] | I_γ (mb) This work |
|------------------|---|------------------------------|
| 1678 | 6.39(7) | 6.26(4) |
| 1681 | 1.32(3) | 1.28(1) |
| 1885 | 15.07(16) | 14.57(9) |
| 1999 | 3.30(4) | 3.15(2) |
| 2521 | 4.48(7) | 4.29(4) |
| 2831 | 1.37(3) | 1.33(1) |
| 3532 | 7.18(9) | 7.13(6) |
| 3678 | 11.66(13) | 11.47(10) |
| 4509 | 13.42(14) | 13.28(11) |
| 5269 | 23.98(24) | 24.03(21) |
| 5298 | 17.05(18) | 17.08(19) |
| 5533 | 15.72(17) | 15.82(15) |
| 5562 | 8.58(10) | 8.67(9) |
| 6322 | 14.64(18) | 14.89(13) |
| 7299 | 7.54(10) | 7.68(8) |
| 8310 | 3.31(7) | 3.34(5) |
| 9149 | 1.19(5) | 1.14(5) |
| 9152 | 0.12(3) | 0.11(5) |
| 10829 | 11.5(5) | – |

not be guaranteed due to missing multipole mixing ratios for many transitions in $^{15}\text{N}_i$. Furthermore, the correction had to be extrapolated above 8 MeV, where theoretical calculations had not been performed [32].

To determine the intensity values of the ^{14}N capture γ rays, each peak area was multiplied by the corresponding inverse efficiency obtained after the iteration. To calculate partial γ -ray production cross sections, we normalized them to the elemental partial γ -ray production cross section value of 0.01452(7) b for the 1885 keV γ ray, recently published by Révay *et al.* [33], which is somewhat lower than the earlier published value by Révay and Molnár [34]. We have to mention that this value is not affected by the new efficiency, because the 1885 keV γ energy is situated in the energy region where the efficiency is unaltered. To obtain the isotopic production cross section, we divided the elemental cross section by the isotopic ratio of ^{14}N , which is 0.99632(7) [15], which provides 0.01457(7) b. The new partial γ -ray cross section values are listed in Table II for the strongest transitions. A comparison between the new intensity values and those of Jurney *et al.* [3] was also carried out. The two sets of intensities were normalized for the 1885 keV transition, and their ratios were calculated; they are plotted in Fig. 4 for the strongest transitions. A systematic discrepancy as a function of energy is seen here between the present and previous results.

The crossing intensity sums were calculated for the new least-squares intensities and for the intensities of Jurney *et al.* [3] and are plotted in Fig. 5, where a systematic

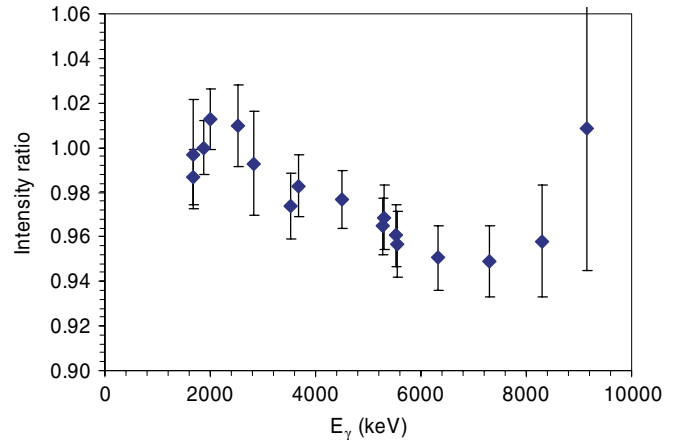


FIG. 4. (Color online) Ratios of intensities for the strongest ^{14}N capture γ rays. Intensities of Jurney *et al.* [3] were divided by intensities from this work. Both data sets were normalized to the 1884 keV intensity.

discrepancy is also seen. While the new fit provides equal intensities for all crossing lines of the considered decay scheme, the CIS values based on the intensities of Jurney *et al.* [3] deviate more and more from unity at lower crossing line numbers. These latter were calculated for the same decay scheme used in the new fit and were normalized to unity at the 16th crossing line, while the values obtained from new CIS fitting were normalized with the fitted constant C [see Eq. (2)]. The deviation at low crossing lines implies missing intensity from the highest energy γ rays, as shown in Fig. 4.

The fit also gives a new cross section for the ^{14}N thermal neutron capture. The constant C provides a means to calculate it. Its value can be renormalized using the intensity of the 1885 keV transition including a correction made for the

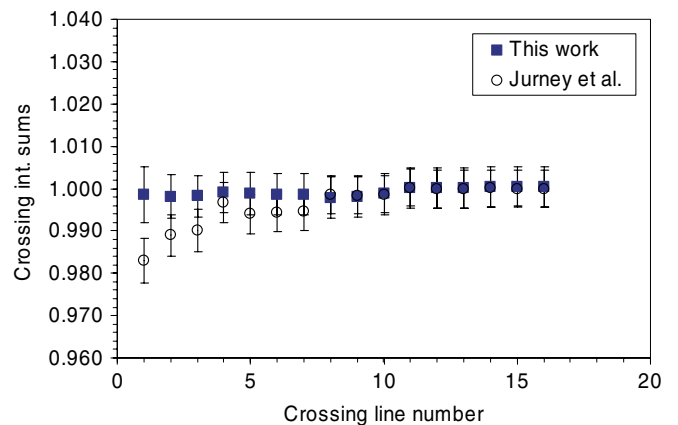


FIG. 5. (Color online) Result of the crossing intensity sum calculations. Filled squares represent the sum of intensities [Eq. (2)] for each crossing line using CIS derived intensities of this work; open circles represent the same sums with the intensity values of Jurney *et al.* [3]. Transitions belonging to the 10 702 and 10 450 keV levels and the primary transition were excluded from both calculations. The summed intensity defined in Eq. (2) was normalized to 1 with fitted parameter C for this work and at the 16th crossing line number for the Jurney *et al.* intensities.

isotopic ratio of ^{14}N . As a result, we obtained 68.77(56) mb for the *total radiative capture cross section of the considered decay scheme*. The uncertainty of this value contains a 0.5% systematic uncertainty added quadratically to the statistical one. The full cross section can only be determined if the partial γ -ray production cross section of the 10 829 keV γ ray is given. However, as we have mentioned, this cannot be determined from our fit. In the literature, the partial γ -ray production cross section of the 10 829 keV γ ray varies between 11 and 14 mb. Based on this range, we can say that the total capture cross section is between 80 and 83 mb, which can overlap with the recently evaluated value of 79.8(14) mb [35] within uncertainties. With the most recent value of 11.5 (5) mb for the partial γ -ray production cross section of the 10 829 keV γ ray proposed by Journey *et al.* [3], we obtain 80.3(8) mb, which agrees well with Mughabghab's evaluated value [35]. Some neglected transitions leading to the proton unstable states should be included, but their effect is only minor on the total capture cross section.

V. DISCUSSION

These new measurements, together with the CIS analysis procedure, give intensity values with higher accuracy and better or similar precision than those of Journey *et al.* [3]. The accuracy is ensured by the constant intensity sums.

The new ^{15}N intensities, when used for detector calibration, will cause changes in the calculated γ -ray intensities of other nuclei, especially at high γ energy. This can be best checked by the reevaluation of crossing intensities and will involve a large amount of work, which has to be and will be done in the future. In particular, the influence of the new ^{15}N intensity values will be quite large for the determination of those neutron-capture cross sections that had been calculated from the sum of partial γ -ray production cross sections de-exciting the capture state [36], which are mostly high-energy γ rays.

It can be clearly seen that the new fit based on the basic principle of CIS provides lower efficiency values at higher energies, starting from about 2.7 MeV, than is obtained from the use of the Journey *et al.* [3] intensities. This difference can be better demonstrated in a plot of the intensity ratios (see Fig. 4). It clearly shows that above 2.7 MeV, the intensities of Journey *et al.* [3] are smaller than the values obtained in this work. In fact, the dependence of the decrease can be well approximated by a linear function starting at a value of 1 at about 2.7 MeV—the last well-established intensities from radioactive sources—and reaching a value of about 0.95 at 6 MeV; then this trend seems to turn back at 7 MeV. However, the decreasing accuracy of the last two points make further statements very speculative.

It can now be seen that a more accurate measurement of the intensity of the 10 829 keV γ ray of $^{14}\text{N}(n, \gamma)$ is essential for any further reduction in the uncertainty of ^{14}N total capture cross section determined from the sum of partial γ -ray production cross sections.

Since a complete decay scheme is a necessary assumption for the use of the CIS method, it can be used as a quantitative test of the completeness of the neutron-capture decay schemes for other nuclei and can be a useful tool in the process of building a decay scheme. Finally, we emphasize again that the basic principle of CIS can be deduced from the intensity balances of the levels, and thus it is equivalent with it. However, it lends itself better to a graphical representation, as shown in Fig. 5, than does the intensity balance of levels.

ACKNOWLEDGMENTS

The author thanks Dr. Zsolt Révay for his continuous interest and help in some of the experiments and Dr. Jesse Weil for critical reading of the manuscript. The author is also grateful for support from the Hungarian Academy of Sciences, the Hungarian National Grant (OTKA T-49253), and the NKTH NAP VENUS05 project.

-
- [1] G. L. Molnár, Z. Révay, and T. Belgya, *Nucl. Instrum. Methods A* **489**, 140 (2002).
 - [2] S. Raman, C. Yonezawa, H. Matsue, H. Iimura, and N. Shinohara, *Nucl. Instrum. Methods A* **454**, 389 (2000).
 - [3] E. T. Journey, J. W. Starner, J. E. Lynn, and S. Raman, *Phys. Rev. C* **56**, 118 (1997).
 - [4] T. J. Kennett, W. V. Prestwich, and J. S. Tsai, *Nucl. Instrum. Methods A* **249**, 366 (1986).
 - [5] H. Takayama, M. Kasaishi, A. Tojo, H. Hayashi, I. Miyazaki, T. Shimizu, M. Shibata, K. Kawade, A. Taniguchi, H. Sakane *et al.*, in *2004 Symposium on Nuclear Data INDC(JPN)-195/U*, edited by Y. T. A. T. Fukahori (JAERI, Tokai, Japan, 2005), p. 222.
 - [6] J. I. Trombka, W. V. Boynton, J. Bruckner, S. Squyres, P. E. Clark, R. Starr, L. G. Evans, S. R. Floyd, T. P. McClanahan, J. Goldsten, R. McNutt, and J. S. Schweitzer, *Nucl. Instrum. Methods A* **422**, 572 (1999).
 - [7] W. V. Boynton, W. C. Feldman, S. W. Squyres, T. H. Prettyman, J. Bruckner, L. G. Evans, R. C. Reedy, R. Starr, J. R. Arnold, D. M. Drake, *et al.*, *Science* **297**, 81 (2002).
 - [8] S. R. Floyd, J. W. Keller, J. P. Dworkin, D. F. R. Mildner, in 35th Lunar and Planetary Science Conference, March 15–19, 2004, League City, Texas, 2004, abstract no. 1361 (unpublished).
 - [9] A. Borella, Ph.D. thesis, University of Gent, 2005, p. 181.
 - [10] A. L. Nichols, *Appl. Radiat. Isot.* **60**, 247 (2004).
 - [11] D. L. Anderson and Z. Kasztovszky, in *Handbook of Prompt Gamma Activation Analysis with Neutron Beams*, edited by G. L. Molnár (Kluwer, Dordrecht, 2004), p. 137.
 - [12] C. M. Baglin, E. Browne, E. B. Norman, G. L. Molnár, T. Belgya, Zs. Révay, and F. Szelecsényi, *Nucl. Instrum. Methods A* **481**, 365 (2002).
 - [13] G. J. McCallum and G. E. Coote, *Nucl. Instrum. Methods* **124**, 309 (1975).
 - [14] IAEA-TECDOC-619, 1991 <http://www-nds.iaea.org/reports-new/tecdocs/iaea-tecdoc-0619.pdf>.
 - [15] R. B. Firestone, G. L. Molnár, and Z. Révay, in *Handbook of Prompt Gamma Activation Analysis with Neutron Beams*, edited by G. L. Molnár (Kluwer, Dordrecht, 2004), p. 395.
 - [16] Z. Elekes, T. Belgya, G. L. Molnár, A. Z. Kiss, M. Csatlós,

- J. Gulyás, A. Krasznahorkay, and Z. Mité, *Nucl. Instrum. Methods A* **503**, 580 (2003).
- [17] S. Raman, private communication, 1991.
- [18] T. Belgya, Z. Révay, P. P. Ember, J. Weil, G. L. Molnár, and S. M. Qaim, in *11th International Symposium on Capture Gamma-Ray Spectroscopy and Related Topics*, edited by J. Kvasil, P. Cejnar, and M. Krťicka (World Scientific, Singapore, 2003), p. 562.
- [19] Z. Révay, T. Belgya, Z. Kasztovszky, J. L. Weil, and G. L. Molnár, *Nucl. Instrum. Methods B* **213**, 385 (2004).
- [20] G. L. Molnár, in *Handbook of prompt Gamma Activation Analysis with Neutron Beams*, edited by G. L. Molnár (Kluwer, Dordrecht, 2004), p. 1.
- [21] P. P. Ember, T. Belgya, J. L. Weil, and G. L. Molnár, *Nucl. Instrum. Methods B* **213**, 406 (2004); P. P. Ember, T. Belgya, J. L. Weil, and G. L. Molnár, *Appl. Radiat. Isot.* **57**, 573 (2002).
- [22] T. Belgya, Zs. Révay, and L. Szentmiklósi in *Proceeding of the 12th International Symposium on Capture Gamma-Ray Spectroscopy and Related Topics, University of Notre Dame, Indiana, 2005*, edited by A. A. Woehr and A. Aprahamian (AIP Melville, New York, 2006), p. 300.
- [23] T. Belgya, Z. Révay, and G. L. Molnár, *J. Radioanal. Nucl. Chem.* **265**, 181 (2005).
- [24] B. Fazekas, T. Belgya, L. Dabolczi, G. Molnár, and A. Simonits, *J. Trace Microprobe Tech.* **14**, 167 (1996).
- [25] B. Fazekas, G. Molnár, T. Belgya, L. Dabolczi, and A. Simonits, *J. Radioanal. Nucl. Chem.* **215**, 271 (1997).
- [26] B. Fazekas, J. Östör, Z. Kiss, A. Simonits, and G. L. Molnár, *J. Radioanal. Nucl. Chem.* **233**, 101 (1998).
- [27] Z. Révay, T. Belgya, P. P. Ember, and G. L. Molnár, *J. Radioanal. Nucl. Chem.* **248**, 401 (2001).
- [28] ENSDF, Evaluated Nuclear Structure Data File, compiled by the International Network of Nuclear Structure and Decay Data Evaluators, NNDC, Brookhaven National Laboratory, 2005.
- [29] E. K. Warburton, J. W. Olness, and D. E. Alburger, *Phys. Rev.* **140**, 1202 (1965).
- [30] L. A. Currie, *Anal. Chem.* **40**, 586 (1968).
- [31] T. Belgya, *J. Radioanal. Nucl. Chem.* **265**, 175 (2005).
- [32] T. Kibedi, T. W. Burrows, M. B. Trzhaskovskaya, C. W. Nestor Jr., in *Proceedings of the 10th International Conference on Nuclear Data for Science and Technology, Santa Fe, New Mexico, Sept. 26–Oct. 1, 2004*, AIP Conf. Proc. No. 769, edited by R. C. Haight, M. B. Chadwick, T. Kawano, and P. Talou (AIP, New York, 2005), p. 268.
- [33] Z. Révay, T. Belgya, and G. L. Molnár, *J. Radioanal. Nucl. Chem.* **265**, 169 (2005).
- [34] Z. Révay and G. L. Molnár, *Radiochim. Acta* **91**, 361 (2003).
- [35] S. F. Mughabghab, INDC(NDS)-440 Distr. PG+R, 2003 (unpublished).
- [36] T. Belgya, G. L. Molnár, Z. Révay, and J. Weil, in *Proceedings of the 10th International Conference on Nuclear Data for Science and Technology, Santa Fe, New Mexico, Sept. 26–Oct. 1, 2004*, AIP Conf. Proc. No. 769, edited by R. C. Haight, M. B. Chadwick, T. Kawano, and P. Talou (AIP, New York, 2005), p. 744.